inorganics

MDPI

Article

The Role of Surface Plasmon Resonance of Gold Nanoparticles for the Enhancement of Second Harmonic Generation of Nonlinear Chromophores

Anu Singh Bisht [1], Khuyen Hoang-Thi [1,2], Isabelle Ledoux-Rak [1,*], Hynd Remita [3], Frédéric Dumur [4], Audrey Guerlin [5], Eddy Dumas [6] and Cédric R. Mayer [6]

1 LPQM, UMR 8537 CNRS, CentraleSupelec, ENS Paris Saclay, 94230 Cachan, France; anu29feb@gmail.com (A.S.B.); khuyenht@ims.vast.ac.vn or khuyenhtims@gmail.com (K.H.-T.)
2 Institute of Materials Science, Vietnam Academy of Science and Technology, 18 Hoang Quoc Viet, Cau Giay, Hanoi 100000, Vietnam
3 Laboratoire de Chimie Physique, UMR 8000-CNRS, Bât 349, Université Paris-Sud 11, 91405 Orsay CEDEX, France; hynd.remita@u-psud.fr
4 Aix Marseille Univ, CNRS, ICR UMR 7273, F-13397 Marseille, France; frederic.dumur@univ-amu.fr
5 Université Paris Diderot, UFR de Chimie, 15 Rue Jean Antoine de Baïf, 75013 Paris, France; Audrey.guerlin@univ-paris-diderot.fr
6 Département de Chimie, UFR des Sciences, Université de Versailles Paris-Saclay, 78035 Versailles CEDEX, France; eddy.dumas@uvsq.fr (E.D.); cedric.mayer@uvsq.fr (C.R.M.)
* Correspondence: isabelle.ledoux@ens-paris-saclay.fr; Tel.: +33-1-47-40-55-60

Received: 16 April 2019; Accepted: 15 May 2019; Published: 18 May 2019

Abstract: A significant enhancement of the second harmonic generation (SHG) from second-order nonlinear optical (NLO) dyes in solution has been evidenced when these dyes were grafted onto the surface of spherical gold nanoparticles (AuNPs), as compared to their NLO response without AuNPs. The length, as well as the nature of the spacers between the gold particle and the chromophore, is shown to play an important role, a benzene linker being more favorable to AuNP-4-dimethylamino-*N*-methyl-4-stilbazolium tosylate (DAST) interactions, as illustrated by a higher exaltation of the NLO response for DAST molecules linked to AuNP via a phenyl ring as compared to their equivalent with a CH_2–CH_2 link.

Keywords: nanoparticles; nonlinear optics; chromophore; plasmonics

1. Introduction

During the past decades, a great effort has been devoted to the synthesis of new materials with large second-order optical nonlinearities because of their potential use in applications such as high bit rate long-distance optical communications, and more generally, optical information processing [1]. The main advantages of organic second-order nonlinear optical (NLO) materials are their high NLO activity, chemical stability, and easy processability [2]. Among organic NLO materials, 4-dimethylamino-*N*-methyl-4-stilbazolium tosylate (DAST) is one of the most studied molecules. Due to its high activity, this organic salt has already been used for high-sensitive electric field sensors [3] and terahertz (THz) wave generation [4].

Gold nanoparticles (AuNPs) are attracting a great deal of attention due to their optical properties related to surface plasmon resonance (SPR), which depends, not only on the metal itself and on its environment, but also on the size and shape of the particle [5,6]. SPR is related to optically induced collective excitations of conduction electrons. A large enhancement is expected for electromagnetic fields through SPR [7]. Surface functionalization of gold nanoparticles with various ligands results in

the generation of nanocomposites exhibiting optical properties with great potential for biological or medical applications [8,9], with the development of ultrasensitive detection and imaging methods, or regarding physical properties, such as magnetism [10] and linear and nonlinear optical properties [11]. It was demonstrated that the NLO activity of small metallic nanoparticles can be enhanced by deviation of the shape of the nanoparticles from a perfect sphere [12].

Various experimental studies have reported on the exaltation of quadratic NLO properties of molecular units by gold nanostructures. Exaltation of second harmonic generation (SHG) from ultrathin dye layers deposited on fractal gold surfaces has been reported [13]. A second harmonic generation (SHG) signal of individual molecules in the presence of very small AuNPs (1 nm) has been evidenced in the context of biological membrane imaging [14]. Large hyperpolarizability (β) values have also been reported for AuNPs in a solution using harmonic light scattering (HLS), a powerful technique to measure the β value of molecules or particles dispersed in solution [7,15–19]. Theoretical studies on SHG properties of gold nanoparticles have been implemented by several authors [20,21].

In this experimental work, highly nonlinear DAST derivatives have been grafted onto the surface of gold nanoparticles by two different linkers and their NLO response was studied and compared.

2. Results

2.1. UV–Visible Spectroscopy

Absorption spectra for all compounds were recorded in *N,N*-dimethylformamide at room temperature, with all samples converted as hexafluorophosphate salts. Spectral data of nongrafted DAST derivatives **1**, **3**, **4**, sets of nanoparticles-dye associations **Au-3** and **Au-4**, and the dye/**Au-SPh** mixture **Au-1** (see their structure in the Materials and Methods) are presented in Table 1 and typical spectra are shown in Figure 1.

Table 1. Maximum absorption wavelength λ_{max} and hyperpolarizabilities λ_{max} per dye unit for dyes **3** and **4**, dye–nanoparticle associations **Au-3** and **Au-4**, nonfunctionalized gold nanoparticles **Au-SPh**, and **Au-1** mixture without link between dye **1** and **Au-SPh**. Hyperpolarizability measurements were performed at 1.64 μm.

Samples	λ_{max} (nm)	B ($\times 10^{-30}$ esu)
3	483	790
4	483	840
Au-3	461, 541	1800
Au-4	474, 533	2380
Au-1	482, 526	1580
Au-SPh	526	260

Electronic absorption spectra of molecules **1–4** showed an intense and broad band in the visible region, corresponding to the π(–NMe_2) → π* (pyridinium) intramolecular charge transfer (ICT) excitation from the –NMe_2 electron donating groups to the pyridinium acceptor moiety. Absorption maxima for the three ligands were centered at 485 nm (**1**, ε = 34,200 L·mol^{-1}·cm^{-1}; **3**, ε = 28,915 L·mol^{-1}·cm^{-1}; **4**, ε = 27,100 L·mol^{-1}·cm^{-1}), which were slightly shifted compared to the maximum observed for DAST (469 nm). These bathochromic shifts of the ICT band were in line with results previously reported in the literature for DAST derivatives bearing aromatic groups in the acceptor moiety [22]. It was attributed to an improvement in the accepting ability of the pyridinium moiety by a stronger electronic deficiency. Study of the electronic absorption spectra of all Au^0 samples revealed full information about the final nanocomposites. For **Au-3** and **Au-4**, the band detected in the spectral range 370–600 nm was resulted from a double contribution, one around 461 nm for **Au-3** and 474 nm for **Au-4** and the second one, with a similar intensity compared to the first band, around 541 nm for **Au-3** and 533 nm for **Au-4**. The first band corresponded unambiguously to ICT band of the chromophores and the second band to the surface plasmon band (SPB) of Au-NPs. A hypsochromic

shift of the ICT band and a bathochromic shift of the SPB were then detected after covalent linkage of the chromophores to Au-NPs. For **Au-1**, the ICT band was not shifted and more intense due to the overlap with the SPB of gold nanoparticles. This result was consistent with a physical mixing of a chromophore with NPs, with the overall observed spectrum corresponding to the addition of the ICT band of the chromophore and the SPB band of the gold particles. For **Au-3** and **Au-4**, only the ligands grafted onto the Au^0 surface were detected and the ICT band was nearly as intense as the SPB band. A similar result has recently been obtained for other organic molecules [23]. A comparison of the SPB position for Au^0-*S-Tolyl* without chromophores (521 nm) with the position observed for **Au-4** (533 nm) and **Au-3** (541 nm) confirmed the anchorage of the chromophores onto the Au^0-NPs surface. The strong interaction between the chromophores and the nanoparticles was also evidenced by the shift of the ICT bands, especially for **Au-3**. It was certainly due to the close proximity of chromophore **3** to the surface.

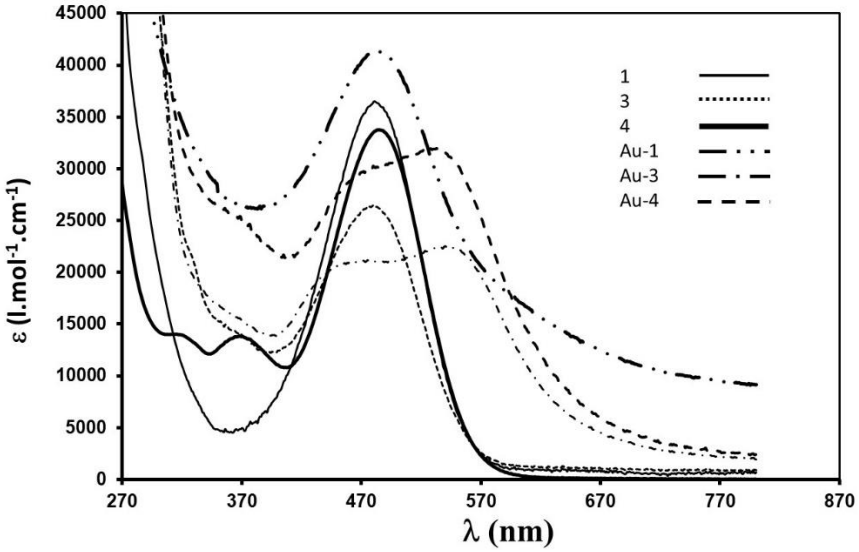

Figure 1. UV–visible absorption spectra of molecules **1** (continuous line), **3** (dotted line), **4** (thick, continuous line), dye-functionalized nanoparticles **Au-3** (dotted-dashed line) and **Au-4** (dashed line), and the **Au-1** sample made of a mixture of **1** and **Au-SPh** without link between dye 1 and gold nanoparticle (double-dotted-dashed line).

2.2. Transmission Electron Microscopy

Transmission electron microscopy (TEM) images of all samples were obtained from the samples analyzed by HLS. No specific aggregation was observed. The TEM images showed an average core diameter of 4 ± 1 nm (Figure 2), consistent with the expectations from the experimental process. The size, shape, and dispersity of gold nanoparticles **Au-1**, **Au-3**, and **4** were similar to those observed for the initial dodecylamine-coated nanoparticles.

2.3. Nonlinear Measurements

We have compared the NLO response of the **Au-3** and **Au-4** composites with a simple mixture of the chromophore and AuNPs without covalent linkers or electrostatic interactions (sample **Au-1**). The results are displayed in Table 1.

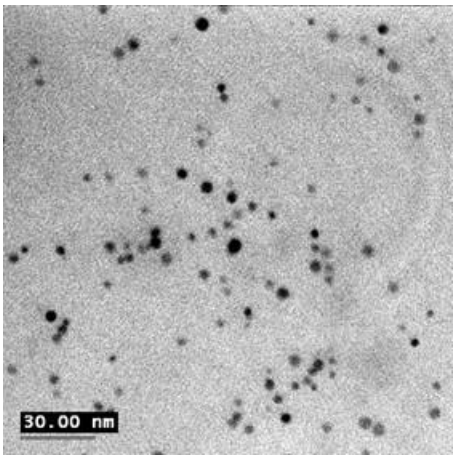

Figure 2. TEM image of Au-SPh nanoparticles; scale bar 30 nm.

3. Discussion

In spite of the fact that the plasmon resonance wavelength of AuNPs lies far from that of the second harmonic signal at 820 nm, we evidenced a clear exaltation factor (by a factor of 3 for **Au-4**) of the hyperpolarizability of stilbazolium derivatives when they were grafted to a gold nanoparticle. The nature of the linker has a significant influence on β value. In spite of the larger distance (about 5.8 Å vs. 3.8 Å for **Au-3**) separating AuNP to the nitrogen atom of the pyridinium moiety in DAST molecule in the case of **Au-4** as compared to **Au-3**, the phenyl group favored the interaction of the chromophore with gold NP compared to the CH_2–CH_2 linker. This behavior does not seem to reflect the expected exponential decrease of I(2ω) after increasing the distance between the dye and the gold surface, as evidenced in Reference [24]. However, our configuration differs from that of [23], as in our case the dye-gold surface distances are very small, and the spacers between the DAST derivative and gold surface are strongly different. In the case of **Au-4**, the π-electrons of the conjugated benzene ring seem to interact significantly with both pyridinium and AuNP electrons, resulting in a higher interaction between DAST and electrons of Au-NP, and hence to a higher exaltation of the NLO response of the DAST derivative, prevailing over the distance effect. A weaker, however, detectable magnification was also observed for a simple mixture of stilbazolium ligand and Au-NPs functionalized with thiophenol (Au-SPh).

4. Materials and Methods

Materials: All reagents were of high-purity grade and used without further purification and purchased from Sigma-Aldrich Chimie (Lyon, France), ACROS Organics (Fisher Scientific, Illkirch, France), and from CLAL (Paris, France).

4.1. Synthesis of AuNPs

AuNPs were synthesized by radiolysis [25]. Radiolysis has proven to be a very efficient technique for the synthesis of nanoparticles of different aspect ratios, controlled size, and morphology. The effect of the interaction of high-energy radiation such as gamma rays with a solution of metals ions induces ionization and excitation of the solvent and leads to the formation of molecular and radical species throughout the solution. The gamma-irradiation source was a ^{60}Co gamma-ray source of 7000 Curies with a dose rate of 1.75 Gys^{-1} (6300 gyh^{-1}) at University Paris Sud. The deposited energy into the irradiated medium is expressed in Grays, 1 Gy = 1 $J{\cdot}kg^{-1}$ (for aqueous solutions, 1 Gy corresponds to 1 $J{\cdot}L^{-1}$).

$HAuCl_4$ and the stabilizer were added to a stirred aqueous solution containing 0.1 M of 2-propanol (added to scavenge HO· radicals). The solutions were bubbled with N_2 before irradiation. Au complexes were homogeneously reduced by solvated electrons and alcohol radicals.

4.2. Functionalization of AuNPs with DAST

A highly active NLO chromophore derived from **2** has been grafted onto the surface of spherical gold nanoparticles by two different linkers and has also been mixed with spherical AuNPs without covalent linker or electrostatic interactions. When the two types of linkers were synthesized, molecule **2** was transformed into a stilbazolium derivative by grafting a mercaptoethyl ethyl group in **3** and a mercaptobenzyl group in **4** (Figure 3). The presence of the SH moiety allowed the functionalization of dye molecules onto the gold surface. Chromophores **3** and **4** were prepared starting from **2** [26] in three and two steps, respectively.

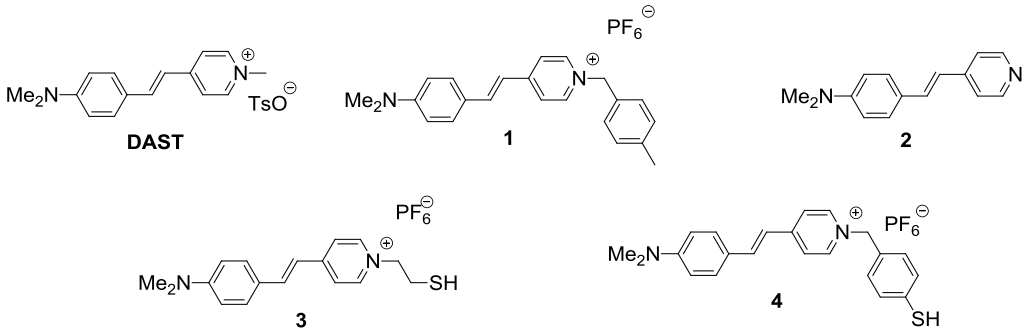

Figure 3. 4-dimethylamino-*N*-methyl-4-stilbazolium tosylate (DAST) derivatives with linkers.

For the chromophore and AuNPs mixture with no specific interactions, we used **1** as this chromophore exhibits a structure similar to **4**. It was synthesized in one step from **2** and *p*-bromomethyl toluene.

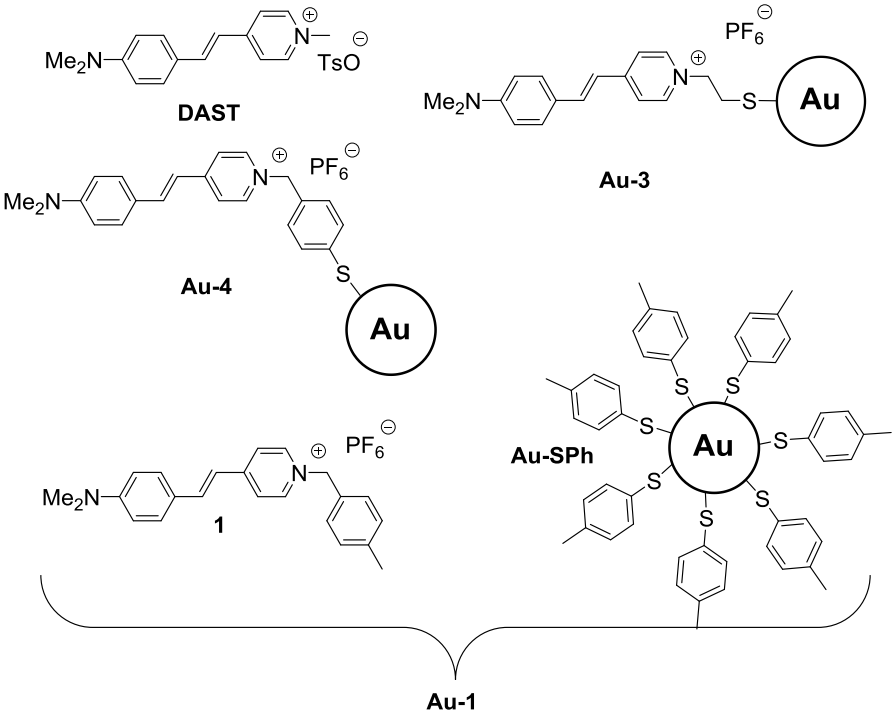

Figure 4. Structures of **Au-3** and **Au-4** functionalized gold nanoparticles (AuNPs) (**top**) and composition of the **Au-1** sample (**bottom**).

In order to obtain gold nanoparticles with similar sizes and shapes to compare NLO coefficients, only one assay of dodecylamine-capped AuNPs was prepared in cooled dichloromethane (DCM) and used during the postfunctionalization step. Monodisperse gold nanoparticles were synthesized in DCM by reduction of a tetrachloroaurate salt ($AuCl_4^-$) with sodium borohydride in the presence of the

stabilizing agent (dodecylamine), according to the procedure of Brust and coworkers [27]. Subsequently, thiol-functionalized gold nanoparticles **Au-3** and **Au-4** were obtained through ligand exchange reaction of the stabilizing agent with molecules **3** and **4** previously dissolved in *N*,*N*-dimethylformamide (DMF). This exchange was facilitated by the weak stabilization ensured by the amine and a stronger affinity of the thiol group for the gold surface. In the third set of Au^0-NPs (**Au-1**), Au^0 surface was first capped with thiophenol by ligand exchange followed by addition of **1**. This addition was done in such a way that the amount of **1** in the assay was similar to that observed for samples **Au-3** and **Au-4**. The final step of the preparation consisted of precipitation of the nanoparticles and their redispersion in DMF, except for **Au-1** for which the solvent was evaporated and the residue dissolved in 5 mL of DMF. The final structures of the samples are shown in Figure 4.

4.3. NLO Experimental Set-Up

The harmonic light scattering (HLS) method at λ = 1640 nm was used for β measurements, because the SH wavelength at 820 nm lies far from 2-photon resonance with the absorption spectra of DAST and Au-NPs. The fundamental beam was emitted by an optical parametric oscillator (OPO) pumped at 355 nm by a frequency-tripled Nd^{3+}: YAG ns laser at a 10-Hz repetition rate. The incident laser beam was passed through a half-wave plate in order to continuously change the incident fundamental intensity between two crossed Glan polarizers. A small part of the incident beam was taken by a glass plate and sent onto a highly nonlinear NPP (*N*-4-nitrophenyl-prolinol) powder used as a reference frequency doubler. The emitted second harmonic signal was detected by a photomultiplier. The NLO measurement set-up is represented in Figure 5.

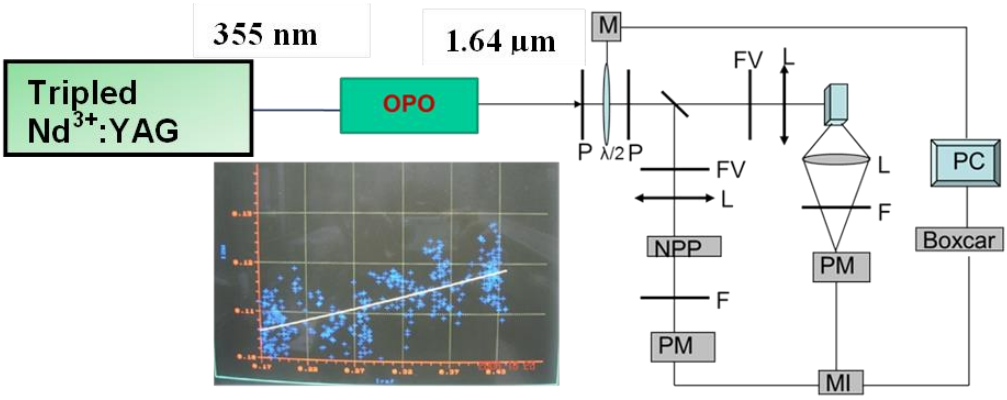

Figure 5. A schematic diagram of HRS measurement at 1.64 µm. F: Filter; M: Mirrors; A: Attenuator; GP: Glass plate; L: Lens; P: Polarizer; λ/2: Half wave plate; PMT: Photomultiplier tube; NPP (*N*-4-nitrophenyl-prolinol): Reference material.

AuNPs functionalized solutions with NLO-dye were placed in a 1 cm long fluorescent cell, at the focus of the incoming fundamental beam. Harmonic incoherent emission was collected in a 90° configuration using two convergent lenses, detected by a photomultiplier, sampled and averaged using a Stanford boxcar integrator, and processed by a computer. The fundamental beam was focused into the fluorescence cell using a 5-cm focal length converging lens. Solutions were preliminary cleaned through 0.45 µm Millipore® filters in order to remove most microscopic particles which could otherwise induce breakdowns in the presence of the focused IR laser beam.

Variation of the scattered second harmonic intensity from the solution is recorded on the computer as a function of the reference second harmonic signal provided by the NPP powder ($I_{NPP}{}^{2\omega}$), which scales like the square of the incoming fundamental intensity I(ω). For a two-component (solvent and analyte) solution, the HLS intensity I(2ω) is given by

$$I(2\omega) = G < N_s \beta_s{}^2 + N_a \beta_a{}^2 > I^2(\omega)\, e^{(-N s \alpha l)} \quad (1)$$

where G is a parameter that accounts for the instrument and local field factors, N_s and N_a is the number of solvent and analyte molecules per unit volume, β_s and β_a is the molecular hyperpolarizability of the solvent and analyte molecule, α is the molar absorption coefficient of the solution, l is the path length of the optical cell, and I(ω) is the intensity of the incident light. To obtain β_a values, it is necessary to work in two steps. First, the second-order intensity of the solvent only is measured as a function of ($I_{NPP}{}^{2\omega}$), giving a slope p_s. The same experiment is then carried out with the solution of analyte, resulting in a slope p_a. Knowing β_S value for the solvent, β_a is determined by calculating the ratio of the two slopes.

5. Conclusions

In this article, we have evidenced the positive role of plasmonic effects in the enhancement of the microscopic nonlinear response of chromophores in the proximity of gold nanoparticles, in spite of the fact that the fundamental and harmonic frequencies are remote from nanosphere plasmonic resonance. These NLO nanostructures offer interesting perspectives in the domain of ultrasensitive detection and imaging methods. Further studies will focus on the influence of the different sizes of AuNRs on the NLO response and functionalization of AuNRs with different NLO dyes.

Author Contributions: Synthesis of chromophores, functionalization on gold nanoparticles, UV–visible spectroscopy: F.D., A.G., E.D., C.R.M.; nonlinear optical measurements: A.S.B., K.H.-T., I.L.-R.; synthesis and TEM characterization of gold nanoparticles: H.R. writing and editing: I.L.-R., C.R.M.

Funding: This research was funded by C'NANO IDF, CNRS, the ANR agency (AURUS program), the PRES UniverSud and the PHOREMOST European Network of Excellence for financial supports.

Conflicts of Interest: The authors declare no conflict of interest. The funders had no role in the design of the study; in the collection, analyses, or interpretation of data; in the writing of the manuscript, or in the decision to publish the results.

References

1. Zyss, J. *Molecular Nonlinear Optics: Materials, Physics and Devices*; Academic Press: Boston, MA, USA, 1994.
2. Nalwa, H.S.; Miyata, S. *Non-Linear Optics of Organic Molecules and Polymers*; CRC Press: Boca Raton, FL, USA, 1997.
3. Nagaoka, K.; Adachi, H.; Brahadeesaran, S.; Higo, T.; Takagi, M.; Yoshimura, M.; Mori, Y.; Sasaki, T. High-quality organic 4-dimethylamino-*N*-methyl-4-stilbazolium tosylate (DAST) crystals for THz wave generation. *Jpn. J. Appl. Phys.* **2004**, *43*, L1121–CL1123. [CrossRef]
4. Suizi, K.; Miyamoto, K.; Yamashita, T.; Ito, H. High-power terahertz-wave generation using DAST crystal and detection using mid-infrared powermeter. *Opt. Lett.* **2007**, *32*, 2885–2887. [CrossRef]
5. Bachelier, G.; Russier-Antoine, I.; Benichou, E.; Jonin, C.; Brevet, P.-F. Multipolar second-harmonic generation in noble metal nanoparticles. *J. Opt. Soc. Am. B* **2008**, *25*, 955–960. [CrossRef]
6. Chen, H.; Kou, X.; Yang, Z.; Ni, W.; Wang, J. Shape- and size-dependent refractive index sensitivity of gold nanoparticles. *Langmuir* **2008**, *24*, 5233–5237. [CrossRef] [PubMed]
7. Russier-Antoine, I.; Benichou, E.; Bachelier, G.; Jonin, C.; Brevet, P.F. Multipolar contributions of the second harmonic generation from silver and nanoparticles. *J. Phys. Chem. C* **2007**, *111*, 9044–9048. [CrossRef]
8. Salata, O.V. Applications of nanoparticles in biology and medicine. *J. Nanobiotechnol.* **2004**, *2*, 3. [CrossRef]
9. Sztandera, K.; Gorzkiewicz, M.; Klajnert-Maculewicz, B. Gold nanoparticles in cancer treatment. *Mol. Pharm.* **2019**, *16*, 1–23. [CrossRef] [PubMed]
10. Guerrero, E.; Munoz-Marquez, M.A.; Garcia, M.A.; Crespo, P.; Fernandez-Pinel, E.; Hernando, A.; Fernandez, A. Surface plasmon resonance and magnetism of thiol-capped gold nanoparticles. *Nanotechnology* **2008**, *19*, 175701. [CrossRef]
11. Butet, J.; Brevet, P.-F.; Martin, O.J.F. Optical second harmonic generation in plasmonic nanostructures: From fundamental principles to advanced applications. *ACS Nano* **2015**, *9*, 10545–10562. [CrossRef] [PubMed]
12. Nappa, J.; Revillod, G.; Russier-Antoine, I.; Benichou, E.; Jonin, C.; Brevet, P.F. Electric dipole origin of the second harmonic generation of small metallic particles. *Phys. Rev. B* **2005**, *71*, 165407. [CrossRef]

13. Anceau, C.; Brasselet, S.; Zyss, J.; Gadenne, P. Local second-harmonic generation enhancement on gold nanostructures probed by two-photon microscopy. *Opt. Lett.* **2003**, *28*, 713–715. [CrossRef] [PubMed]
14. Peleg, G.; Lewis, A.; Linial, M.; Loew, L.M. Non-linear optical measurement of membrane potential around single molecules at selected cellular sites. *Proc. Natl. Acad. Sci. USA* **1999**, *96*, 6700–6704. [CrossRef]
15. Terhune, R.W.; Maker, P.D.; Savage, C.M. Measurements of nonlinear light scattering. *Phys. Rev. Lett.* **1965**, *14*, 681–684. [CrossRef]
16. Clays, K.; Persoons, A. Hyper-rayleigh scattering in solution. *Phys. Rev. Lett.* **1991**, *66*, 2980–2983. [CrossRef]
17. Johnson, R.C.; Li, J.; Hupp, J.T.; Schatz, G.C. Hyper-rayleigh scattering studies of silver, copper, and platinum nanoparticle suspensions. *Chem. Phys. Lett.* **2002**, *356*, 534–540. [CrossRef]
18. Galletto, P.; Brevet, P.F.; Girault, H.H.; Antoine, R.; Broyer, M. Size dependence of the surface plasmon enhanced second harmonic response of gold colloids: Towards a new calibration method. *Chem. Commun.* **1999**, *7*, 581–582. [CrossRef]
19. Ngo, H.M.; Nguyen, P.P.; Ledoux-Rak, I. Optimization of second harmonic generation of gold nanospheres and nanorods in aqueous solution: The dominant role of surface area. *Phys. Chem. Chem. Phys.* **2016**, *18*, 3352–3356. [CrossRef] [PubMed]
20. Xiong, H.; Si, L.-G.; Ding, C.; Yang, X.; Wu, Y. Second-harmonic generation of cylindrical electromagnetic waves propagating in an inhomogeneous and nonlinear medium. *Phys. Rev. E* **2012**, *85*, 016606. [CrossRef]
21. Xiong, H.; Si, L.-G.; Guo, J.-F.; Lu, X.-Y.; Yang, X. Classical theory of cylindrical nonlinear optics: Second-harmonic generation. *Phys. Rev. A* **2011**, *83*, 063845. [CrossRef]
22. Coe, B.J.; Harris, J.A.; Asselberghs, I.; Clays, K.; Olbrechts, G.; Persoons, A.; Hupp, J.T.; Johnson, R.C.; Coles, S.J.; Hurthouse, M.B.; et al. Quadratic nonlinear optical properties of *N*-aryl stilbazolium dyes. *Adv. Funct. Mater.* **2002**, *12*, 110–116. [CrossRef]
23. Mayer, C.R.; Dumas, E.; Michel, A.; Sécheresse, F. Gold nanocomposites with rigid fully conjugated heteroditopic ligands shell as nanobuilding blocks for coordination chemistry. *Chem. Commun.* **2006**, *40*, 4183–4185. [CrossRef] [PubMed]
24. Ishifuji, M.; Mitsuishi, M.; Miyashita, T. Bottom-up design of hybrid polymer nanoassemblies elucidates plasmon-enhanced second harmonic generation from nonlinear optical dyes. *J. Am. Chem. Soc.* **2009**, *131*, 4418–4424. [CrossRef] [PubMed]
25. Belloni, J.; Mostafavi, M.; Douki, T.; Spotheim-Maurizot, M. *Radiation Chemistry: From Basics to Applications in Material and Life Sciences*; EDP Sciences: Paris, France, 2008; pp. 97–116.
26. Pepitone, M.F.; Jernigan, G.G.; Melinger, J.S.; Kim, O.K. Synthesis and characterization of donor–acceptor chromophores for unidirectional electron transfer. *Org. Lett.* **2007**, *9*, 801–804. [CrossRef] [PubMed]
27. Kanaras, A.G.; Kamounah, F.S.; Schaumburg, K.; Kiely, C.J.; Brust, M. Thioalkylated tetraethylene glycol: A new ligand for water soluble monolayer protected gold clusters. *Chem. Commun.* **2002**, *20*, 2294–2295. [CrossRef]